ASEG-PESA 2013
'THE EUREKA MOMENT'
11-14 AUGUST 2013 • MELBOURNE, AUSTRALIA

Coal seismic diffraction fault imaging: Results from numerical modelling

Weijia Sun
Institute of Geology and Geophysics
Chinese Academy of Sciences, Beijing, China
swj@mail.iggcas.ac.cn

Binzhong Zhou
CSIRO Earth Science and Resource Engineering
PO Box 883, Kenmore, QLD 4069
Binzhong.Zhou@csiro.au

Peter Hatherly
Coalbed Geoscience Pty Ltd
10 Waiwera St, McMahons Point. NSW 2006
geophys@bigpond.com.au

Li-Yun Fu
Institute of Geology and Geophysics
Chinese Academy of Sciences, Beijing, China
lfu@mail.iggcas.ac.cn

SUMMARY

Faults are the most important geological structures which need to be detected in any modern underground coal mining project. Even a fault with a throw of a few metres can create safety issues and lead to costly delays in mine production. While locating faults with throws greater than 5-10m is quite successful by seismic survey, techniques to resolve the more subtle faults, shears and features, which exploration programs should also locate are needed.

Faults cause breaks in continuity of seismic horizons. These discontinuities generate diffraction patterns. Before the days of seismic migration and generation of very high fold data, diffraction patterns were sought by seismic interpreters as an indication of faulting, especially for small faults where the discontinuities of the seismic reflections are less evident. Most processing is now aimed at suppressing these diffractions. However, in recent years, techniques for diffraction imaging developed for petroleum seismic data processing, makes small fault detection possible by separating the diffraction events from the reflection seismic events.

In this paper, we apply the diffraction imaging techniques to enhance the detectability of the small faults for coal seismic environments and demonstrate the feasibility of a new fault imaging method with numerical examples. The effects of noise and migration velocity to fault imaging will also be discussed.

Key words: Fault detection, diffraction imaging.

INTRODUCTION

Modern underground coal mining requires certainty about geological faults and other structural features for safety reasons. Even a fault with a throw of a few metres can create safety issues and lead to costly delays in mine production. To ensure there are no unwelcome surprises concerning seam conditions during mining, seismic reflection surveys have been widely used by Australian coal mines, due to their unprecedented ability to detect geological structures. While locating faults with throws greater than 5-10 m can be done using seismic surveys, the ability to resolve the more subtle faults, shears and features that exploration programs should also locate is still a challenge in the coal mining industry (Zhou and Hatherly, 2012).

There are two types of seismic energies that can be used for subsurface imaging: reflections and diffractions. Reflections are created by the smooth surfaces such as continuous coal seams, while diffractions are caused by the discontinuities such as faults, pinchouts and fractures. Therefore, it is possible to use diffractions to image faults. Prior to using seismic migration, seismic interpreters sought diffraction patterns as an indication of faulting structures, especially for small faults where the discontinuities in the seismic reflections are less evident. These diffractions are often attenuated by conventional seismic data processing (Khaidukov et al., 2004; Bansal and Imhof, 2005; Moser and Howard, 2008). However, the significance of these diffractions has been long recognised in fault and other discontinuity imaging by many researchers such as Krey (1952), Hagedoorn (1954), Trorey (1970), Harlan et al. (1984), Landa et al. (1987), Kanasewich and Phadke (1988), Neidell (1997), Khaidukov et al (2004), Shtivelman and Keydar (2004) and Landa (2010). Many approaches and applications have been developed for diffraction imaging. The key applications of diffractions are for detections of faults and fractures (Khaidukov et al., 2004; Cheng and Hilterman, 2007; Al-Dajani and Fomel, 2010; Zhu and Wu, 2010) and migration velocity analysis (Harlan et al., 1984; Soellner, and Yang, 2002; Sava et al., 2005; Fomel et al., 2007; Landa and Fomel, 2008; Reshef and Landa, 2009). Many good numerical examples have been reported but successful real data examples are scarce.

Currently, all the reported examples are petroleum exploration oriented, where targets are relatively deep and the seismic frequencies are relatively low around 10 – 60 Hz. In this paper, we apply the diffraction imaging techniques to enhance the detectability of small faults for coal seismic environments and demonstrate the feasibility of a new fault imaging method with numerical examples. In addition, the effects of noise and velocity will also be discussed.

FAULT IMAGING BY DIFFRACTIONS

The most important step in diffraction fault imaging is to extract or separate diffractions from reflections. However, this requires care because the energy of diffracted events is generally one or two orders of magnitude weaker than that of specular reflections (Klem-Musatov, 1994; Reshef and Landa, 2009). Many approaches have been proposed to achieve the separation needed. Harlan et al (1984) and Fomel et al. (2007) proposed the local slant stack (plane wave decomposition, τ-p

transform) for separating diffractions from reflections for velocity estimation on post-stack sections. Khaidukov et al. (2004) and Berkovitch et al. (2009) extracted the diffractions by muting the focused imaginary source points from reflections on a prestack shot gather. Taner et al. (2006) used plane-wave destruction filter to suppress reflections and retain diffractions. Landa and Fomel (2008), Reshef and Landa (2009) and Klokov and Fomel (2012) adopted the hybrid Radon transform (Trad et al, 2001) to separate reflections and diffractions using their shape differences in the migrated dip-angle domain. Bansal and Imhof (2005) examined several workflows to enhance diffractions and suppress reflections in the normal-moveout (NMO)-corrected prestack data. Seven approaches are tested, including Diote and dip filtering on common-offset gathers, dip filtering for NMO-corrected shot-gathers, NMO-dip-moveout filtering, eigenvector (Singular-value decomposition – SVD) filtering and Harlan signal/noise separation and Radon filtering.

On the basis of our testing, f-k dip filtering on NMO-corrected common-shot gathers (Bansal and Imhof, 2005) is probably the most effective method for extracting diffractions from specular reflections. Theoretically, after applying NMO corrections, the reflected events are flattened (or sub-flattened) and the diffracted events are deformed. We can then use a dip filter to suppress flattened reflections by muting the data with the spatial wavenumber k close to 0. Due to its simplicity, fast computation and effectiveness, we can use this approach to extract diffractions. The following is a summary of the workflow for diffractions fault imaging:

1) Pre-processing including trace editing and static corrections;
2) Sorting shot gathers into CMP gathers, and making velocity analysis on CMP gathers using reflections;
3) NMO-correcting the CMP gathers to flatten reflections;
4) Re-sorting the NMO-corrected CMP gathers into common shot gathers;
5) Transforming the NMO-corrected shot gathers into the f-k domain;
6) Extracting diffractions from reflections by muting the data near-zero k-value in the f-k domain;
7) Inverse-transforming the extracted diffractions from the f-k domain back to the x-t space;
8) Re-sorting the extracted-diffraction shot gathers back to the CMP gathers;
9) Inverse-NMO-corrections to restore the traveltime to the original state;
10) Sorting the extracted diffraction data back to shot domain;
11) Prestack-depth-migrating the shot gathers with diffractions and generating a prestack migration image.

RESULTS

Geological model

Synthetic seismic data is used to demonstrate the feasibility of enhancing small fault detection by diffraction imaging. A geological model with acoustic velocity distribution in Figure 1 was used for this purpose. This is a multi-layered model with 3 coal seams and many small faults with throws between 1 and 20m. The actual fault model is defined by a 2D grid of 801×401 points with a grid spacing of 1m in both directions. The seismic data (shot gathers) were simulated using an acoustic finite-difference method. The source is a Ricker wavelet with a peak frequency of 100 Hz, and the time sampling interval is 0.1ms. The shots and receivers are placed on the surface with a shot interval of 10m and a receiver interval of 5m. There are 61 shot gathers in total with 161 traces in each shot record. A typical shot gather at surface shot location of 360m is presented in Figure 2. The synthetic seismic shot gather was computed by solving the acoustic wave equation using a finite difference method (Virieux, 1984). The direct, reflected and diffracted waves can be easily identified from the record. The diffractions can be seen to be much weaker than the reflections.

Diffraction extraction from shot gathers

The shot record in Figure 2 is used to illustrate the procedures of diffraction extraction from shot gathers. This is shown by Figure 3. Figure 3(a) is the NMO-corrected shot record, which flattens the reflections and under-corrects the diffractions, which maintain a hyperbolic moveout. If the data is converted into the f-k domain using fast Fourier transform (FFT), the flattened reflections will be concentrated around the frequency axis with the spatial wavenumber k=0 (Zhou and Greenhalgh, 1994). Therefore, we can attenuate the reflections by muting the data around k=0. Figure 3(b) gives the extracted diffractions after f-k filtering. Figure 3(c) shows the shot gather with extracted diffractions after restoration to the original travel times using inverse NMO corrections. It is clear that the diffractions have been largely extracted. This illustrates the effectiveness of the f-k dipping filtering in separating the diffractions from the reflections.

Diffraction fault imaging

Figure 4 shows an example of fault imaging by using Fourier finite-difference (FFD) prestack depth migration (Ristow and Ruhl, 1994). Figure 4(a) shows the imaging result with original data containing both reflections and diffractions using the true velocity model in Figure 1 while Figure 4(b) presents the result with the data containing only the extracted diffractions. These results illustrate that small faults (1-3m) are not easily detectable by conventional processing but they are detectable through this diffraction imaging approach. Note also that while this method indicates the locations of faults, throws are not revealed. To determine throws, conventional seismic sections should be studied.

Effect of random noise

Given that the magnitude of the diffractions is much smaller than the reflections, diffracted events can be easily contaminated by noise. To investigate this, we added random Gaussian noise into the raw shot gathers and followed the same workflow to produce diffraction images.

Figure 5(a) shows the same shot record as in Figure 2 but with added relatively strong Gaussian noise with a signal-to-noise ratio (S/N) of 10. The diffractions are barely observable on this plot due to the noise. Figure 5(b) is the result after extracting the diffractions by suppressing the reflections using the f-k filtering. Compared with the result in Figure 3(c), the diffractions are much weaker. Figure 6 is the depth migration result from the shot gathers with the extracted diffractions, which corresponds to Figure 5(b). Although the section is nosier, all the fault points are still evident. This was expected because migration, as a summation process, is able to suppress random noises.

Effect of migration velocity

The previous results were generated with the true migration velocity. In a practical situation, the actual velocity distribution is not precisely known and errors in the velocity model are unavoidable. To test for the effect of the migration velocity, we applied our method using velocities which were 90% and 110% of the true velocity model. The results are presented in Figure 7. The faults have still been located but it can be seen that locations are incorrect with those with the lower velocity under-migrated (Figure 7(a) and those with the higher velocity over-migrated (Figure 7(b)). However, this example does illustrate the robustness of this approach.

CONCLUSIONS

Instead of ignoring or suppressing diffractions by conventional seismic data processing, they can be used for the identification of geological discontinuities such as faults, pinch-outs, and small-size scattering objects. In this paper, we have separated the diffractions from reflections with the aid of NMO-corrections and f-k dip filtering of pre-stack shot gathers. It has been demonstrated that the extracted diffractions can be used to identify small faults that are difficult to detect using conventional seismic reflection processing. Numerical examples demonstrate that the diffractions can be used to identify faults with a throw of 1m, even in a moderately noisy environment and when the migration velocities are not accurate. This clearly shows that this approach is robust.

ACKNOWLEDGMENTS

This research was supported by the Australian Coal Association Research Program (ACARP) and the Natural Science Foundation of China (Grant No. 41104079).

REFERENCES

Al-Dajani, A., and S. Fomel, 2010, Fractures detection using multi-azimuth diffractions focusing measure: Is it feasible?: 80th Annual International Meeting, SEG, Expanded Abstracts, 287–291.

Bansal, R., and Imhof, M., 2005, Diffraction enhancement in prestack seismic data: Geophysics, 70,V73-V79.

Berkovitch, A., Belfer, I., Hassin, Y., and Landa, E., 2009, Diffraction imaging by multifocusing: Geophysics, 74, WCA75-WCA81.

Cheng, M., and Hilterman, F., 2007, Scattering object imaging with azimuthal binning to detect vertical fractures: Extended abstract, SEG Meeting, 2045-2049.

Fomel, S., Landa, E. and Taner, T., 2007, Poststack velocity analysis by separation and imaging of seismic diffractions: Geophysics 72, U89–U94.

Hagedoorn, J. G., 1954, A process of seismic reflection interpretation: Geophysical Prospecting, 2, 85–127.

Harlan, W., Claerbaut J., and Rocca, F. 1984, Signal to noise separation and velocity estimation: Geophysics 49, 1869–1880.

Kanasewich, E., and Phadke, S., 1988, Imaging discontinuities on seismic sections: Geophysics, 53, 334–345.

Khaidukov, V., Landa, E., and Moser, T.J., 2004, Diffraction imaging by focusing-defocusing: An outlook on seismic superresolution: Geophysics, 69, 1478–1490.

Klem-Musatov, K., 1994, Theory of seismic diffractions: SEG.

Klokov, A., and Fomel, S., 2012, Separation and imaging of seismic diffractions using migrated dip-angle gathers: Geophysics, VOL.77, NO.6, S131-S143.

Krey, T., 1952, The significance of diffraction in the investigation of faults: Geophysics, 17, 843–858.

Landa, E., 2010, Diffractions – Yesterday, today and tomorrow: 72nd EAGE Conference & Exhibition incorporating SPE EUROPEC 2010, Barcelona, Spain, 14 - 17 June 2010.

Landa, E., and Fomel, S., 2008, Separation, imaging, and velocity analysis of seismic diffractions using migrated dip-angle gathers: 78th Annual International Meeting, Expanded Abstracts, 2176-2180.

Landa, E., Shtivelman, V., and Gelchinsky, B., 1987, A method for detection of diffracted waves on common offset sections: Geophysical Prospecting. 35, 359–374.

Moser, T., and Howard, C. B., 2008, Diffraction imaging in depth: Geophysical Prospecting, 56, 627–641.

Neidell, N. S., 1997, Perceptions in seismic imaging, Part 2: Reflective and diffractive contributions to seismic imaging: The Leading Edge, 16, 1121–1123.

Reshef, M., and Landa, E., 2009, Post-stack velocity analysis in the dip-angle domain using diffractions: Geophyscial Propsecting, 57, 811-821.

Ristow, D., and Ruhl, T., 1994, Fourier finite-difference migration: Geophysics, 59, 1882–1893.

Shtivelman, V., and Keydar, S., 2004, Imaging shallow subsurface inhomogeneities by 3D multipath diffraction summation: First Break, 23, 39–42.

Sava P., Biondi B., and Etgen, J., 2005, Wave-equation migration velocity analysis by focusing diffractions and reflections: Geophysics 70, U19–U27.

Soellner,W., and Yang, W., 2002, Diffraction response simulation:A3D velocity inversion tool: 72nd Annual International Meeting, SEG, Expanded Abstracts, 2293–2296.

Taner, M. T., S. Fomel, and E. Landa, 2006. Prestack separation of seismic diffractions using planewave decomposition: SEG, Expanded Abstracts, 2401–2404.

Trad, D., M. Sacchi, and T. Ulrych, 2001, A hybrid linear-hyperbolic Radon transform: Journal of Seismic Exploration, 9, 303–318.

Trorey, A.W., 1970, A simple theory for seismic diffractions: Geophysics, VOL.35, NO.5, 762-784.

Virieux, J., 1984, SH-wave propagation in heterogeneous media: velocity-stress finite difference method: Geophysics, 49, 1933-1942.

Zhou, B., and Greenhalgh, S.A., 1994, Wave-equation extrapolation-based multiple attenuation: 2_D filtering in the f-k domain: Geophysics, V.59, NO.9, 1377-1391.

Zhou, B., and Hatherly, P., 2012, Seismic fault detectability: a view from numerical modelling: 22nd ASEG International Geophysical Conference and Exhibition, Brisbane, 26-29 February 2012.

Zhu, X., and Wu, R., 2010, Imaging diffraction points using the local image matrices generated in prestack migration: Geophysics, V.74 NO.1, S1-S9.

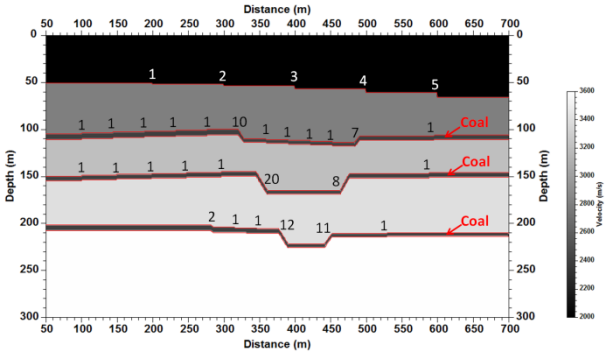

Figure 1 A velocity model with multi-layers, 3 coal seams and many faults. The fault throw ranges from 1m to 20m as labelled on the plot. The red lines represent the layer boundaries.

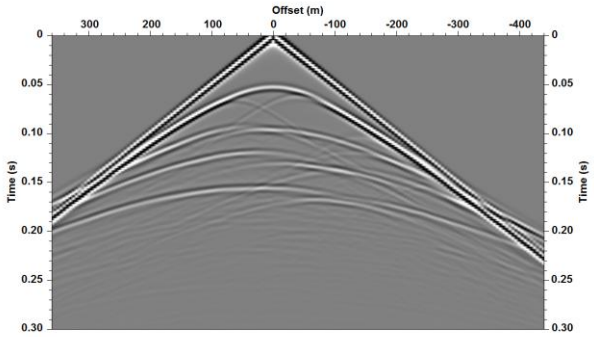

Figure 2 A synthetic shot record at the source position of 360m shown in the model in Figure 1. The direct arrival, reflections and diffractions can be easily observed.

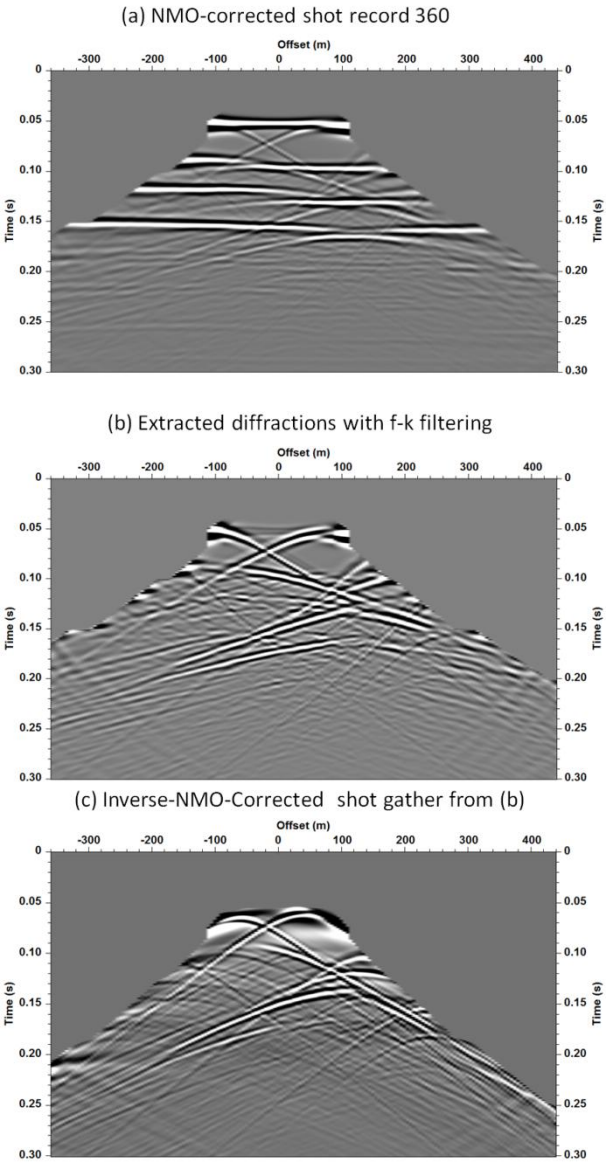

Figure 3 Extracting diffractions from the shot record in Figure 2: (a) the NMO-corrected shot record; (b) extracted diffractions from (a) using f-k filtering; (c) the shot record with diffractions only after inverse NMO correction.

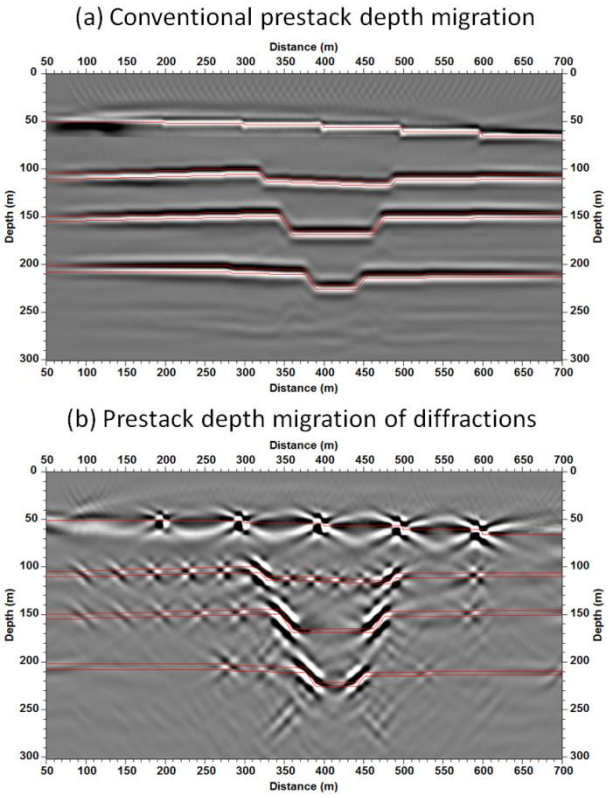

Figure 4 Pre-stack Fourier finite-difference (FFD) depth migration: (a) with reflections and diffractions; (b) with only the extracted diffractions. All the 1m throw faults are clearly imaged by the diffraction imaging.

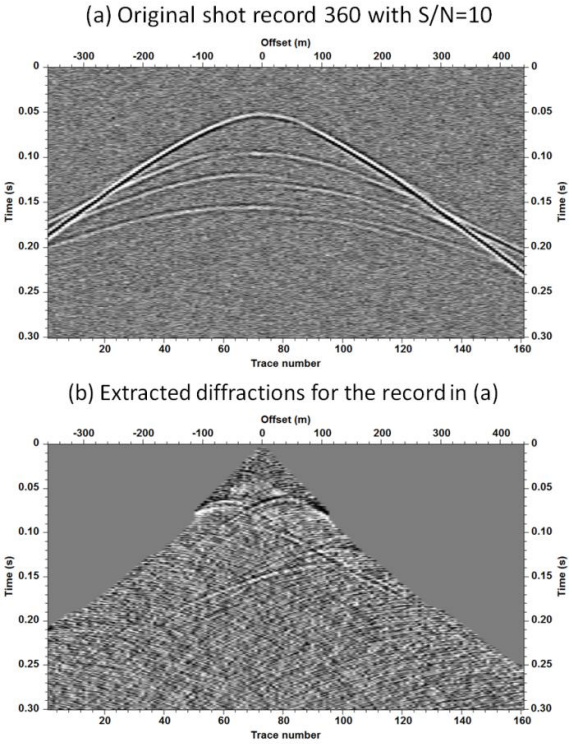

Figure 5 The same shot record in Figure 3 (a) with random noise added: (a) the original shot record with a S/N=10; (b) the extracted diffractions from the record in (a). Direct waves have been removed on this plot.

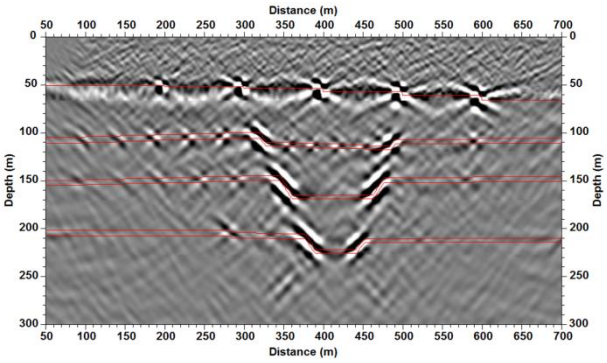

Figure 6 The diffraction fault image from the seismic data with a S/N=10. The faults are all clearly imaged in spite of the noise.

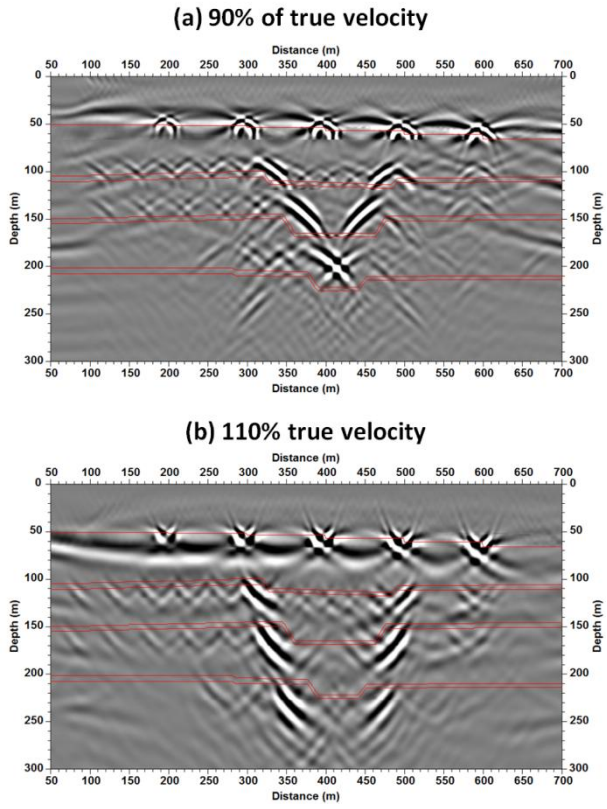

Figure 7 The effect of migration velocity on diffraction fault imaging: (a) with 90% of true velocity; (b) 110% of true velocity.